THE JOURNAL OF COMPARATIVE NEUROLOGY 359:490–506 (1995)

Human Cingulate Cortex: Surface Features, Flat Maps, and Cytoarchitecture

BRENT A. VOGT, ESTHER A. NIMCHINSKY, LESLIE J. VOGT, AND PATRICK R. HOF
Department of Physiology and Pharmacology, Bowman Gray School of Medicine, Wake Forest University, Winston-Salem, North Carolina 27157-1083 (B.A.V., L.J.V.) and Fishberg Research Center for Neurobiology & Department of Geriatrics and Adult Development, Mount Sinai School of Medicine, New York, New York 10029-6574 (E.A.N., P.R.H.)

ABSTRACT

The surface morphology and cytoarchitecture of human cingulate cortex was evaluated in the brains of 27 neurologically intact individuals. Variations in surface features included a single cingulate sulcus (CS) with or without segmentation or double parallel sulci with or without segmentation. The single CS was deeper (9.7 ± 0.81 mm) than in cases with double parallel sulci (7.5 ± 0.48 mm). There were dimples parallel to the CS in anterior cingulate cortex (ACC) and anastomoses between the CS and the superior CS. Flat maps of the medial cortical surface were made in a two-stage reconstruction process and used to plot areas. The ACC is agranular and has a prominent layer V. Areas 33 and 25 have poor laminar differentiation, and there are three parts of area 24: area 24a adjacent to area 33 and partially within the callosal sulcus has homogeneous layers II and III, area 24b on the gyral surface has the most prominent layer Va of any cingulate area and distinct layers IIIa–b and IIIc, and area 24c in the ventral bank of the CS has thin layers II–III and no differentiation of layer V. There are four caudal divisions of area 24. Areas 24a′ and 24b′ have a thinner layer Va and layer III is thicker and less dense than in areas 24a and 24b. Area 24c′ is caudal to area 24c and has densely packed, large pyramids throughout layer V. Area 24c′g is caudal to area 24c′ and has the largest layer Vb pyramidal neurons in cingulate cortex. Area 32 is a cingulofrontal transition cortex with large layer IIIc pyramidal neurons and a dysgranular layer IV. Area 32′ is caudal to area 32 and has an indistinct layer IV, larger layer IIIc pyramids, and fewer neurons in layer Va. Posterior cingulate cortex has medial and lateral parts of area 29, a dysgranular area 30, and three divisions of area 23: area 23a has a thin layer IIIc and moderate-sized pyramids in layer Va, area 23b has large and prominent pyramids in layers IIIc and Va, and area 23c has the thinnest layers V and VI in cingulate cortex. Area 31 is the cinguloparietal transition area in the parasplenial lobules and has very large layer IIIc pyramids. Finally, variations in architecture between cases were assessed in neuron perikarya counts in area 23a. There was an age-related decrease in neuron density in layer IV ($r = -0.63$; ages 45–102), but not in other layers. These observations provide structural underpinnings for interpreting functional imaging studies of the human medial surface.

Indexing terms: cerebral cortex, limbic cortex, cingulate gyrus, human imaging, sulcal patterns

Brodmann's (1909) cytoarchitectural map of the cerebral cortex has been used as the standard for human brain research. The distribution of areas on the cingulate gyrus in this account, however, does not have the same level of detail as do other assessments of human cingulate cortex and recent nonhuman primate studies. von Economo (1929), for example, reported that area LA (Brodmann's area 24) and area LC (Brodmann's area 23) were not uniform but that each contained three dorsoventral subdivisions. In addition, Braak identified an anterogenual magnocellular area rostral to the genu of the corpus callosum (1979) and a primitive gigantopyramidal area in the depths of the cingulate sulcus (1976), both of which may be divisions of area 24. The concept that a sulcal part of area 24 contains a cingulate motor area has been elaborated in nonhuman primate studies of the cingulospinal projections (Biber et al., 1978; Dum and Strick, 1991, 1993), electrically evoked movements (Luppino et al., 1991), premotor unit discharge properties (Shima et al., 1991), and corticocortical connec-

Accepted March 16, 1995.

Address reprint requests to Brent A. Vogt, Department of Physiology and Pharmacology, Bowman Gray School of Medicine, Medical Center Boulevard, Winston-Salem, NC 27157-1083.

tions (Morecraft and Van Hoesen, 1992; Bates and Goldman-Rakic, 1993) of this region.

The rostral and caudal parts of area 24 have cytoarchitectural, connectional, and functional differences. Variations in cytoarchitecture were incorporated into an analysis of the rhesus monkey where the anterior division was designated area 24 and the caudal division area 24′ (Vogt, 1993). This report also emphasized a number of differences in the connections of these areas including the heavy projection of the amygdala to area 24 and light projection to area 24′ and greater projections from parietal cortex to area 24′ than to area 24. An assessment of these areas is needed in the human brain.

Positron emission tomography (PET) studies of blood flow also suggest that perigenual area 24 is distinct from the caudal part of area 24. The caudal part of area 24, but not perigenual cortex, has been activated with the Stroop interference task and other behavioral response selection paradigms using letter or word generation (Peterson et al., 1988; Pardo et al., 1990), complicated finger movement sequences (Schlaug et al., 1994) and self-generated eye movements (Petit et al., 1993), pain (Jones et al., 1991; Talbot et al., 1991; Casey et al., 1994), and divided attention tasks (Corbetta et al., 1991). By contrast, George et al. (1993) reported an elevation in blood flow in rostral area 24 associated with pictures of faces that had intense emotional expressions and, in another study, showed that anterior areas 24 and 25 had altered blood flow during internal imaging of sad life experiences (George et al., 1995). A review of the contributions of different parts of human anterior cingulate cortex to behavior considers these issues in some detail (Devinsky et al., 1995). In view of the functional heterogeneity of cingulate cortex, a thorough assessment of the cytoarchitecture of the human cingulate gyrus is necessary so that functional imaging and other studies of human brain can take into account the unique features of each division of cingulate cortex.

The structural and functional heterogeneity of human cingulate cortex must be considered in the context of the substantial variation in sulcal patterns on the medial surface. This variability in sulcal patterns has been documented in postmortem samples by Retzius (1896) and Ono et al. (1990) and include the number of cingulate sulci (CS) and their segmentation, as well as variations in the distribution of the superior rostral sulcus and its anastomoses with the CS. Furthermore, the cytoarchitecture of this region needs to be defined within the context of medial cortex variations. For example, in the case used by Brodmann (1909) the CS is closely apposed to the callosal sulcus at the level of the genu, and area 24 is almost nonexistent. This implies either that most of Braak's (1979) anterogenual magnocellular area is area 32 or, if it is part of area 24, that it has a limited extent in this brain. Thus, not only are there variations in the surface features of the human cingulate gyrus, these variations provide an important context for assessing its cytoarchitectural fields.

The present study was undertaken to reassess the cytoarchitecture of human cingulate cortex from the perspective of recent structural and functional observations and place it in the context of variations in surface morphology. The analysis of cingulate cortex surface features focuses on a simple and consistent nomenclature, variations in the depths of the CS, and identification of the parasplenial lobules. Furthermore, since convolution of the cortical surface results in a large proportion of cortex being buried in the depths of the sulci, this has lead to misrepresentations of the distribution of areas on the medial surface. A methodology was developed whereby flat maps could be derived from individual cases and used to represent the distribution of these areas. Finally, a thorough description of the cingulate cytoarchitectural fields and their location on the human cingulate gyrus is presented as is the extent to which laminar architecture can vary between cases.

MATERIALS AND METHODS

Case material and tissue preparation

Cases employed in this study were from neurologically intact individuals who had no evidence of vascular damage or other neuropathological findings. In one case there was a small brainstem infarct that was not deemed significant to an assessment of cerebral cytoarchitecture. There were three groups of cases used for these studies. The first and largest group consisted of 20 cases for assessing variations in medial surface features and developing a logical nomenclature. The characteristics of this group were as follows: 72 ± 2.7 years of age; 20 ± 8.3 hr postmortem interval (PMI); ten men and ten women; 13 left and 7 right hemispheres; causes of death—cancer (n = 5), congestive heart failure (n = 9), pneumonia (n = 4), and unknown causes (n = 2). The second group of 11 cases was a subset of the first for which the entire cingulate cortex was available for histological analysis (i.e., in some of the first group there were cases with only posterior blocks available). The characteristics of this group were as follows: 70 ± 14.3 years of age; 10.9 ± 2.2 hr PMI; seven men and four women; four right and seven left hemispheres; causes of death—cancer (n = 3), congestive heart failure (n = 4), pneumonia (n = 3), and unknown causes (n = 1). The third group of cases comprised cases with blocks of posterior cingulate cortex (PCC) at the level of the splenium of the corpus callosum. There was no requirement that there be an entire cingulate cortex available in these cases, since they were used only to assess cytoarchitectural variability within area 23. There were 13 cases, of which 6 were also in groups 1 and 2. These 13 cases had the following characteristics: 73.5 ± 3.9 years of age; 8.0 ± 1.9 hr PMI; five men and eight women; causes of death—cancer (n = 6), congestive heart failure (n = 6), and pneumonia (n = 1).

The brains were bisected and the medial surface of each photographed for use in later reconstructions. In one instance this view was not available, since the case was prepared with both hemispheres joined. In some instances the brains were evaluated first for neuropathology with 2-cm coronal sections. The medial surfaces of these cases were dissected and the medial surface reconstructed for photography. Coronal blocks of 2–6-cm thickness were dissected and the brains photographed again so that sections from each block could be identified. The blocks were postfixed in formalin for 1–2 months. For the second group of cases, blocks from eight cases were sectioned into ten consecutive series on a freezing microtome. Sections from four series were 100 μm thick and those from six series were 50 μm thick. Blocks from four cases were embedded in celloidin as previously described (Vogt, 1976). These cases were from younger individuals (60.5 ± 10.3 years), since the preservation of neuron morphology was better with such preparations, and they were used for photomicrography. These cases were cut in ten series at 35 μm or 60 μm, or at 50 μm or 100 μm series of parallel thicknesses. Frozen

sections were mounted on chrome-alum subbed slides and stained with thionin, while celloidin-embedded sections were stained free floating with cresyl violet, mounted, and coverslipped. For the third group of cases, all blocks were sectioned with the freezing microtome and stained as described above.

Analytical and reconstruction techniques

Sections from each case were drawn at 10× with an Aus Jena projector that was modified from microfiche projecting to that for viewing histological slides. Series of 10× photomicrographs were taken through the entire cingulate gyrus and adjacent cortex for three celloidin-embedded cases. Higher magnification photographs were taken selectively throughout the cingulate cortices of these and two frozen cases. These cases were chosen for age (45–75 years), quality of sections, and Nissl staining. Each case was reviewed microscopically to ascertain that each conclusion about regional and laminar structure was consistent for all cases.

Illustrations for this article were prepared in the following manner. The photographic negatives were scanned with a high-resolution flat bed, transilluminating scanner (Microtek, Redondo Beach, CA). These digitized images were imported, composited, and labeled with Adobe Photoshop software (3.0.1, Adobe Systems, Inc., Mountain View, CA). When the final illustration was labeled, the digital files were printed directly with the Fujix Pictography 3000 system (Fuji Photo Film Co, Ltd, Elmsford, NY). This processing resulted in direct printing of illustrations without the need for intermediate printing and labeling and subsequent copy negative and printing for publication.

The medial surface photographs for each case were copied into line drawings to assess surface features. One-third of the transverse sections in a single series were drawn at 17× with an Aus Jena projector. Each transverse section was used to make the first-stage linear expansion of the flat maps, as described below. They were also used to plot the borders of each cytoarchitectural area. This was done by evaluating each section microscopically at 40–200× and placing the border on previously drawn sections. Since celloidin embedding produced less than 7% shrinkage as determined by block lengths before and after embedding, no corrections were made for shrinkage. The area borders were transferred to the flat map so that the topographical distribution of each area could be related to the gross morphology of the cingulate gyrus.

Interindividual variations in cytoarchitecture were determined in area 23a for 13 cases. The perisplenial level of PCC was used because the splenium of the corpus callosum provides a uniform landmark for selecting the level of area 23 to be analyzed. Perikaryal drawings were made with a drawing tube attachment to the microscope. The drawings were made for 160-μm-wide strips of cortex at a final magnification of 320×. Only perikarya with a nucleus and nucleolus were drawn, whereas those for glia and endothelial cells were not drawn. Three samples were taken from each case through area 23a and the average number of neurons in each layer determined. The laminar borders were determined at a low magnification of 40× and marked on the strips of perikarya. The mean ± SEM number of neurons was then calculated for each layer for all cases. These counts were also used to determine whether or not there was an influence of age on neuron densities. This was done by performing correlations between age at death and neuron density in each layer. The significance of the Pearson product-moment correlation coefficient from 0 was estimated with GB-Stat software (Dynamic Microsystems Inc, Silver Spring, MD).

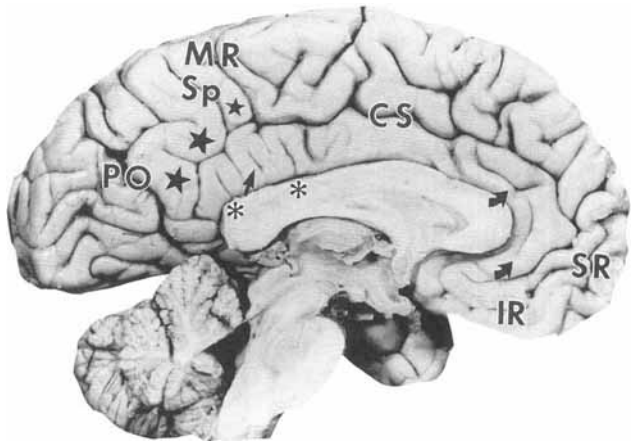

Fig. 1. Medial surface of a case (woman, 75 years old) with parallel secondary sulci in the anterior cingulate cortex (ACC; curved arrows), a vertical dimple in the posterior cingulate cortex (PCC; straight arrow), and two vertical branches of the callosal sulcus (asterisks). The parasplenial lobules in this and the next figure are indicated with stars. CS, cingulate sulcus; IR, inferior rostral sulcus; MR, marginal ramus of the CS; PO, parietooccipital sulcus; Sp, splenial sulcus; SR, superior rostral sulcus.

RESULTS

Surface features of the cingulate gyrus

The most consistent sulcus on the medial surface is the CS and its marginal ramus, which forms the caudal border of the paracentral lobule. In the case illustrated in Figure 1, the CS is uninterrupted and stretches from a point rostral to the paraolfactory sulcus to its termination in the marginal ramus. In anterior cingulate cortex (ACC) the sulci inferior and rostral/superior to the CS are termed the inferior rostral and superior rostral sulci, respectively. In posterior cingulate cortex (PCC), the splenial sulcus lies between the marginal ramus and parietooccipital sulcus; it is vertically oriented, and it extends from medial parietal cortex to PCC. In this case the splenial sulcus anastomoses with the CS. Adjacent to the splenial and parietooccipital sulci are cortical folds or parasplenial lobules (Fig. 1, parasplenial lobules, stars).

In addition to sulci on the medial surface, there are a number of superficial dimples or secondary sulci. These structures are similar to the small free sulci of Ono et al. (1990); they are not simply shallow depressions formed by large blood vessels. The case shown in Figure 1 emphasizes the differences between primary and secondary sulci (curved arrows). In all cases there are a variable number of vertical dimples in PCC as well as branches of the posterior sulci. In Figure 1 there are vertical branches of the cingulate and splenial sulci, two branches of the callosal sulcus (asterisks), and a single, isolated secondary sulcus (straight arrow).

Three additional medial surfaces are given in Figure 2 to show the range of variability in sulcal patterns noted in these 20 cases. The four patterns and their percent frequency in 20 cases is as follows: 1) single CS (40%); 2)

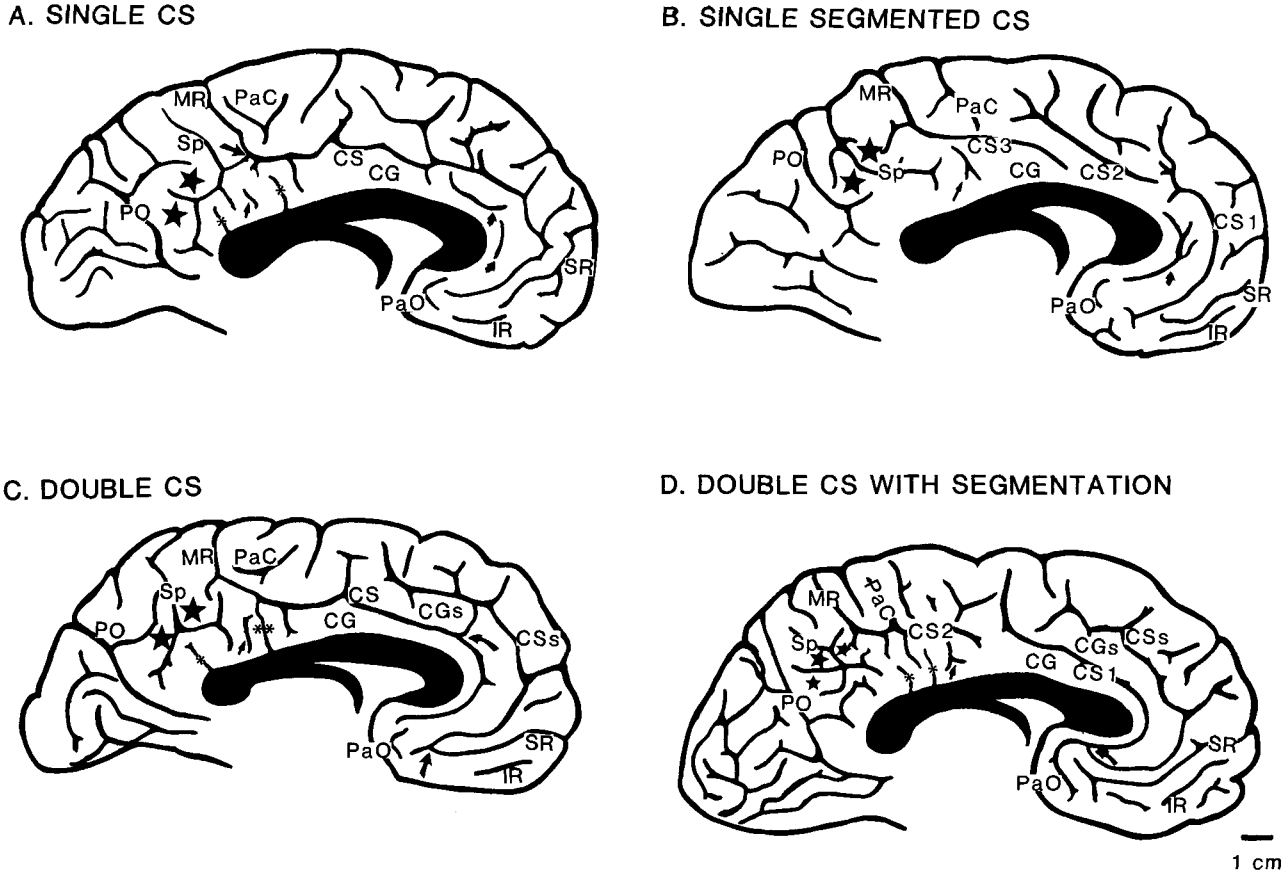

Fig. 2. Medial surface features of the left hemispheres of four cases. **Case A** (also Fig. 1): Continuous cingulate sulcus (CS) and secondary sulci in anterior (curved arrows) and posterior (asterisks and small arrow) cortices. **Case B** (woman, 45 years old): A three-segment cingulate sulcus (CS1, CS2, CS3) and one parallel dimple in ACC (curved arrow). **Case C** (woman, 80 years old): A continuous CS that forms a double parallel pattern with a superior CS (CSs); both are joined (curved arrow). In PCC there is one vertical dimple (small arrow), a vertical branch of the CS, a vertical extension of the callosal sulcus (asterisk), and an anastomosis between the cingulate and callosal sulci (double asterisk). **Case D** (man, 61 years old): A two-part CS and the rostral segment (CS1) anastomoses with the CSs (curved arrow). CG, cingulate gyrus; CGs, superior cingulate gyrus; PaC, paracentral sulcus; PaO, paraolfactory sulcus. For other abbreviations, see legend to Figure 1.

single, segmented CS (25%); 3) double CS (15%); or 4) double CS with segmentation (20%). The second case has a CS that is composed of three segments, and there is a prominent parallel dimple. Retzius (1896) showed the only known example of four segments of the CS in his sample of 100 cases. The third case in Figure 2 is an example of the double parallel distribution of cingulate sulci described by Retzius (1896) and Ono et al. (1990). The CS approaches close to the ventral border of the genu of the corpus callosum and there is a second CS termed the superior cingulate sulcus (CSs). This sulcus arises just rostral to its junction with the superior rostral sulcus (Fig. 2C, large, straight arrow), and it courses parallel to and anastomoses with the CS (curved arrow). Ono et al. (1990) referred to this sulcus as the posterior segment of the CS. This designation is not used here in order to avoid confusion associated with the posterior segment being located in ACC. The dual cingulate sulci form two cingulate gyri in ACC; the ventral one is the main cingulate gyrus and the one between the two cingulate sulci the superior cingulate gyrus (CGs). The fourth case in Figure 2 has a CS that is segmented, the rostral part (CS1) approaches close to the genu of the corpus callosum, and the CSs branches from the CS1 (Fig. 2D, curved arrow). In PCC there is a rich array of vertical sulcal branches and a vertical dimple (small straight arrow). Finally, in all cases there are lobules rostral and caudal to the Sp, which are the parasplenial lobules. These lobules are of particular note because they are comprised of the cingulo-parietal transition area 31.

The cingulate sulci in the single or double parallel patterns are not the same depth. The depth of the CS when there is only one suclus is 9.7 ± 0.81 mm, whereas the depth in double parallel cases is 7.5 ± 0.48 mm ($P = 0.05$). Figure 3 shows an example of a transverse section from a similar rostrocaudal level of a case representing each pattern of sulci. Even when a horizontal secondary sulcus is in ACC of a case with a single sulcus, the cingulate sulcus is deeper than in the double parallel cases.

Flat map rendering of the medial cortical surface

Since about half of the cortex on the medial surface is buried in the depths of sulci, it is not possible to display the topography of cortical areas onto drawings of the convoluted medial surface. An example of the extent to which

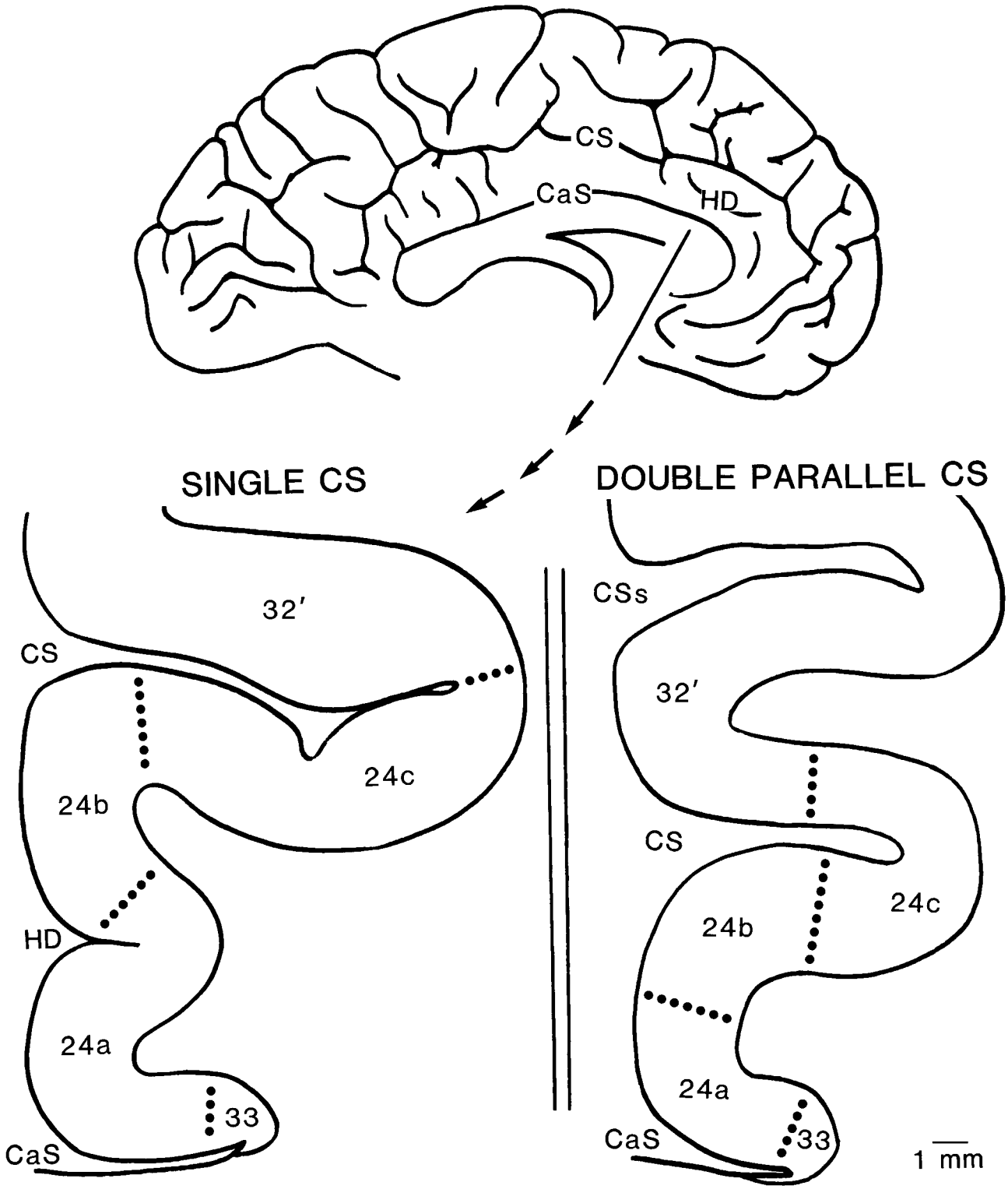

Fig. 3. Drawings of coronal sections through a similar level of ACC from two cases with different sulcal patterns. The first (also Fig. 2A) has a single cingulate sulcus (CS) and horizontal dimples (HD), and the second is from another case with a double parallel pattern of sulci. Notice the different depths of the CS in each case and differences in the size and distribution of the cytoarchitectural areas. CaS, callosal sulcus.

cortex is buried in the CS is shown in Figure 4B, where a coronal section is presented with cortex in the depths of the sulci (crosshatched). This latter cortex cannot be represented on the surface feature drawing. In order to provide a more accurate assessment of the distribution of areas on the medial surface, a two-stage flattening procedure was

employed to produce a flat map rendering of this cortex. The first step consisted of placing fiducial marks at midcortical depths at the apices of each gyrus and the depths of each sulcus (Fig. 4B). There were a total of 275 fiducial marks used for transforming the convoluted surface on 50 coronal sections through cingulate cortex into a flat map. Once the fiducials were marked, the depth of the callosal sulcus provided a consistent starting point for reconstruction, and the fiducials were expanded successively to form a straight line. In the crosshatched region of the linear expansion, it can be seen that cortex in the depths of the sulci comprises more than half of the cortex in this section. The fiducials for the depths of the sulci were connected with dashed lines and those associated with the apices of gyri connected with solid lines. A reconstruction of the expanded coronal sections is shown in Figure 4C. Although the resulting reconstruction is accurate in the ventral-dorsal orientation, the distance between transverse sections was maintained at a constant interval along the full length of the corpus callosum. This resulted in a distortion of the surface area of the gyri, particularly in PCC where sulci and their branches were frequently oriented perpendicular to the corpus callosum, necessitating a second flattening procedure.

In the second stage of flattening a rostrocaudal expansion was made wherever there was a prominent vertical sulcus and in cortex rostral to the corpus callosum. For example, at the level of the marginal ramus, the cortical surface was extended caudally for a distance that was equivalent to the depths of the rostral and caudal banks of this sulcus. This procedure did not include secondary sulci in PCC, since they were relatively superficial and did not appear to delimit cytoarchitecturally unique areas. In order to preserve the integrity of the gyral surface, the expansion was made by bending the corpus callosum at those points where there was a prominent perpendicular sulcus. Thus, as the cortex was expanded to account for the depths of the marginal ramus, the surface of the cingulate gyrus ventral to it was not further expanded. This second stage of flattening was repeated four times. After each reconstruction, the cortex on the surface of the gyrus was compared with that on the unfolded cortical surface. Each subsequent approximation was performed to reduce differences in the area of cortex on gyral surfaces on the flattened and convoluted views. This rostrocaudal expansion procedure resulted in a flattened medial surface that approximated the two-dimensional features of the medial surface. This flat map provides a surface for locating the distribution of cytoarchitectural areas on the gyral surface and in the depths of the sulci.

Topography of the cingulate areas

A number of generalizations about the distribution of areas on the cingulate gyrus can be made with reference to Figure 5 before describing the cytoarchitectural details for each area. The surface of the anterior cingulate gyrus is composed of areas 25 and 24. In the depths of the rostral callosal sulcus is area 33. Surrounding the rostral and dorsal borders of areas 25 and 24 is the cingulofrontal transition area 32. As discussed below, the transition areas are mixtures of cytoarchitectural features of cingulate cortex and adjacent frontal or parietal areas. Whether or not these are strictly cingulate or frontal/parietal areas cannot be determined without substantially more functional studies and some means of evaluating axonal connections in the human brain.

The distributions of the CS and parallel dimples in the perigenual region are variable. In the medial view of the brain depicted by Brodmann (1909), the CS closely approaches the callosal sulcus, area 24 almost disappears rostral to the genu, and the most anterior portion of the cingulate sulcus delineates areas 24 and 32. An evaluation of a number of brains suggests a different organizational pattern. When the CS closely approaches the callosal sulcus, it separates areas 24a and 24b rostral to the genu. When there are dimples parallel to the CS, these secondary sulci usually delineate areas 24a and 24b. Finally, when the CS is distant from the callosal sulcus and there are no parallel dimples, no macroscopic markers are available for delineating areas 24a and 24b.

In light of the above observation that the CS is deeper in cases with a single sulcus than in cases with a double parallel pattern, it should be noted that the distribution of areas is influenced by these differences in sulcal patterns. In Figure 3 the areas are delineated on transverse sections from similar rostrocaudal levels of anterior cingulate cortex for these two sulcal patterns. In the example of the single sulcus, areas 24a, 24b, and 24c are each longer in the dorsoventral plane than they are in the case with the double parallel sulci. In all cases evaluated so far, area 32′ always begins in the depths of the CS. Area 24c does not appear on the gyral surface unless the CS is segmented. Notice in the double parallel case in Figure 3 that area 24c arches around to include almost half of the dorsal bank of the CS. Finally, most of the areas that surround cingulate cortex in the frontal, parietal, and occipital lobes are designated according to Brodmann (1909). The one exception is for areas that comprise supplementary motor cortex. Vogt and Vogt (1919) identified two divisions of this region, with area 6aα adjacent to primary motor cortex and 6aβ rostral to area 6aα. Matelli et al. (1991) characterized two areas in the monkey supplementary motor area; one has some Betz neurons (area F3), and one has no Betz neurons and denser and larger pyramidal neurons in layer IIIc (area F6). There also is functional evidence for a distinction between these areas in the monkey (Luppino et al., 1991). Since a similar cytoarchitecture occurs in human brain, the original designations of Vogt and Vogt (1919) are employed in the present study.

In PCC retrosplenial areas 29 and 30 are buried in the depths of the callosal sulcus. Area 23 is located on the caudal one-third of the cingulate gyrus and extends into the caudal part of the cingulate sulcus before it arches to form the marginal ramus. Area 31 is a cingulo-parietal transition area that has characteristics of both cortical regions. The parasplenial lobules are a useful landmark for identifying where area 31 is located caudal to area 23c and dorsal to area 23b.

Cytoarchitecture of anterior cingulate cortex

Anterior cingulate cortex is agranular and in most instances has a prominent layer Va. The two least differentiated areas in the anterior cingulate region are areas 33 and 25 and they have a slender layer Va. Area 33 lies adjacent to the ventrorostral part and dorsal half of the corpus callosum. It is a periallocortex that abuts the indusium griseum and has almost no laminar organization. Layers II–III are not differentiated and there is almost no layer VI. Only a limited number of large neurons in layer Va provide a clue as to its laminar structure (Fig. 6). Area 25 lies ventral and caudal to area 33. Area 25 has a clearly defined layer V that merges with layer VI. The distinction between layers V and

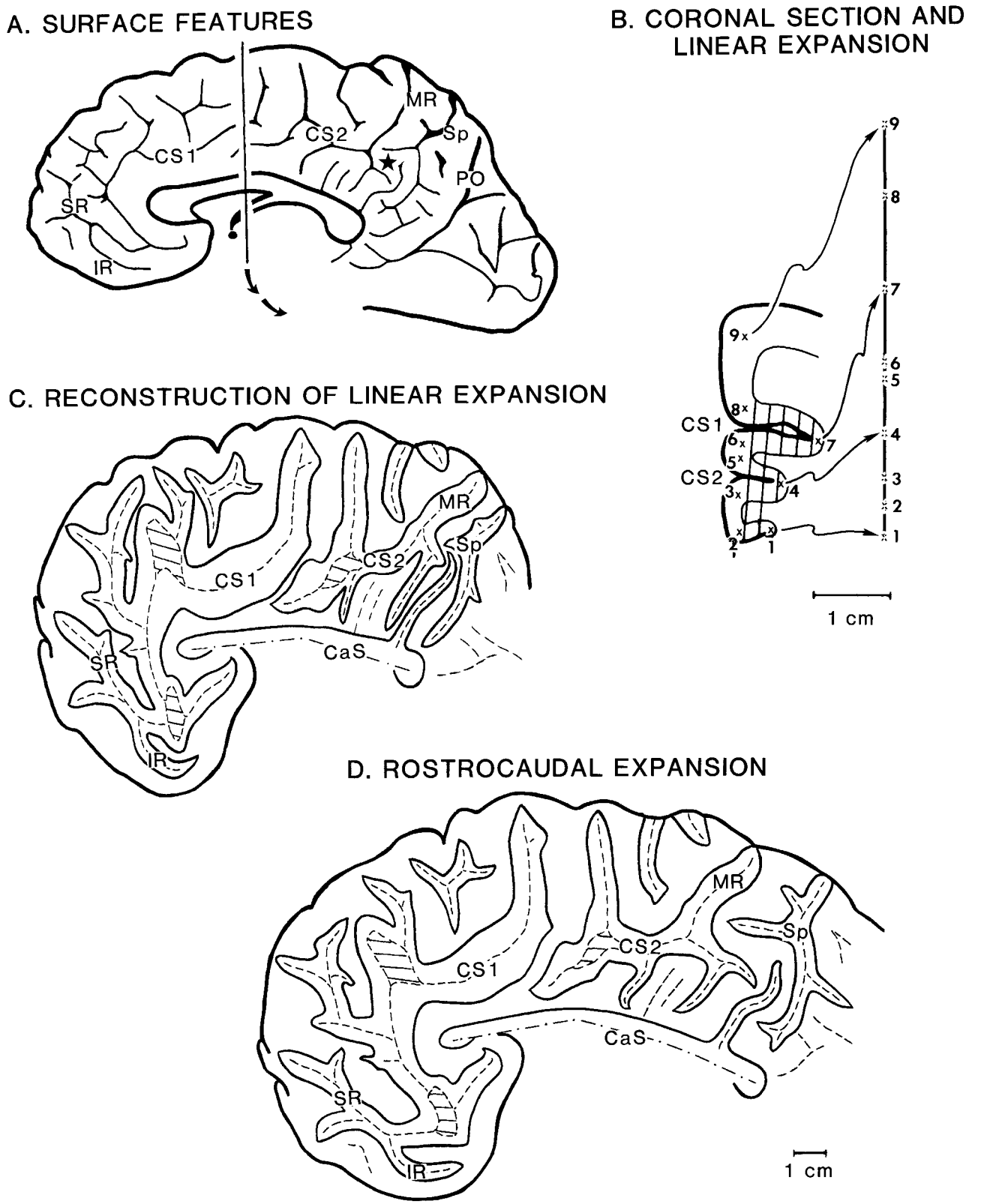

Fig. 4. Medial surface features (**A**) and flat map reconstruction of a case (man, 62 years old) with a two-segment cingulate sulcus (CS: CS1 and CS2). **B:** An example of a coronal section, and the same section expanded. Cortex in the depths of the cingulate sulci is shown with crosshatching. The matched fiducials (#1–9) are shown for the curved and linear versions of this section. In the reconstruction of the linear expansion, the depths of the sulci are indicated with dashed lines and the abbreviations are the same as in Figure 1. **C,D:** The three regions in the depths of the CS (crosshatched) are regions of cortical expansion or cortical insulettes. In ACC the superior rostral sulcus fuses with the CS and the inferior rostral sulcus fuses with the superior branch. A parasplenial lobule is formed at a confluence between a horizontal branch of the CS, the splenial sulcus, and a vertical branch of the callosal sulcus (star in A).

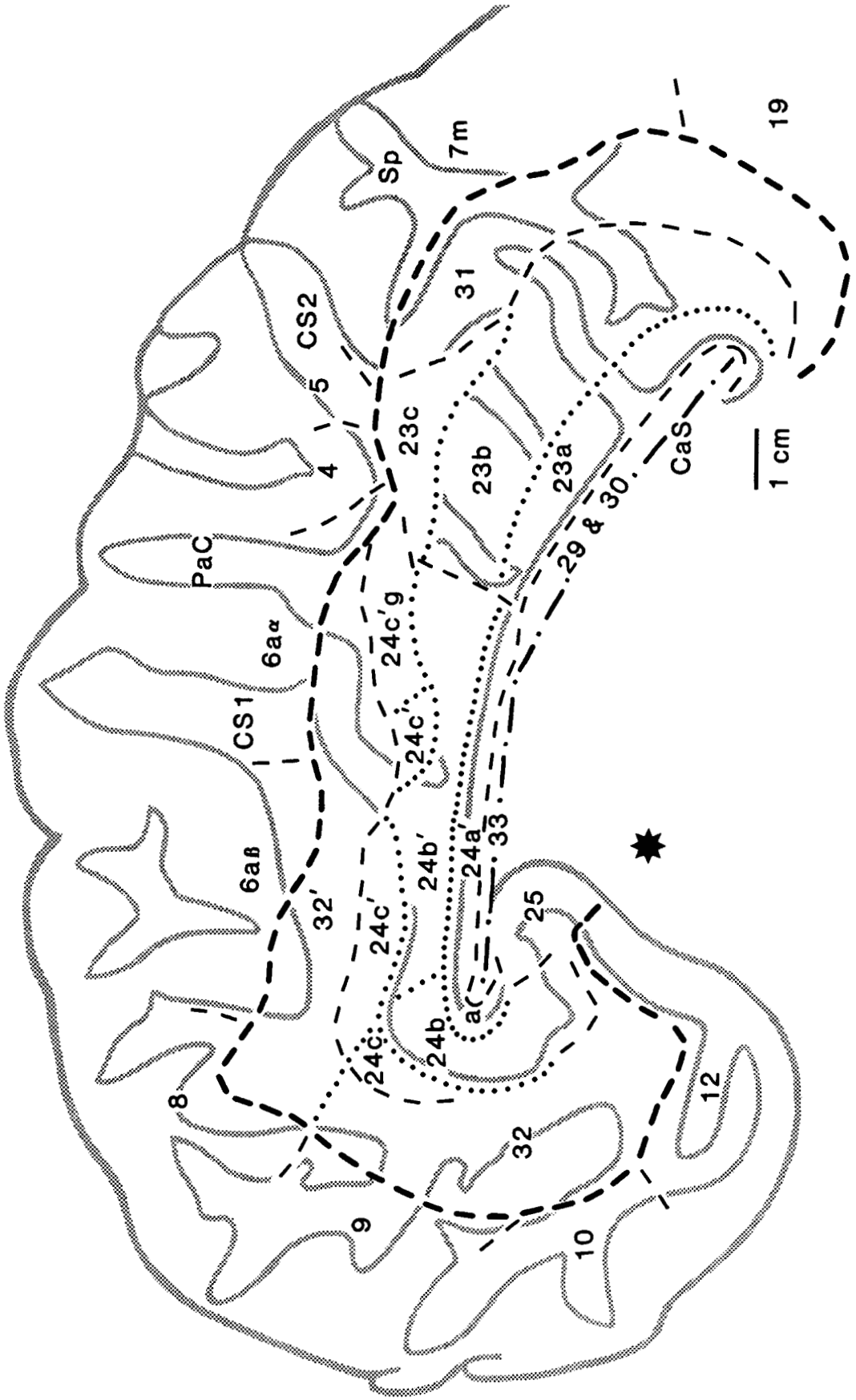
Sp
7m
19
CS2
31
5
4
23c
23b
23a
CaS
1 cm
PaC
29 & 30
6aα
24c'g
CS1
24c'
6aß
32'
24b'
24a'
33
24c'
25
24b
a
24c
8
12
32
9
10

Figure 5

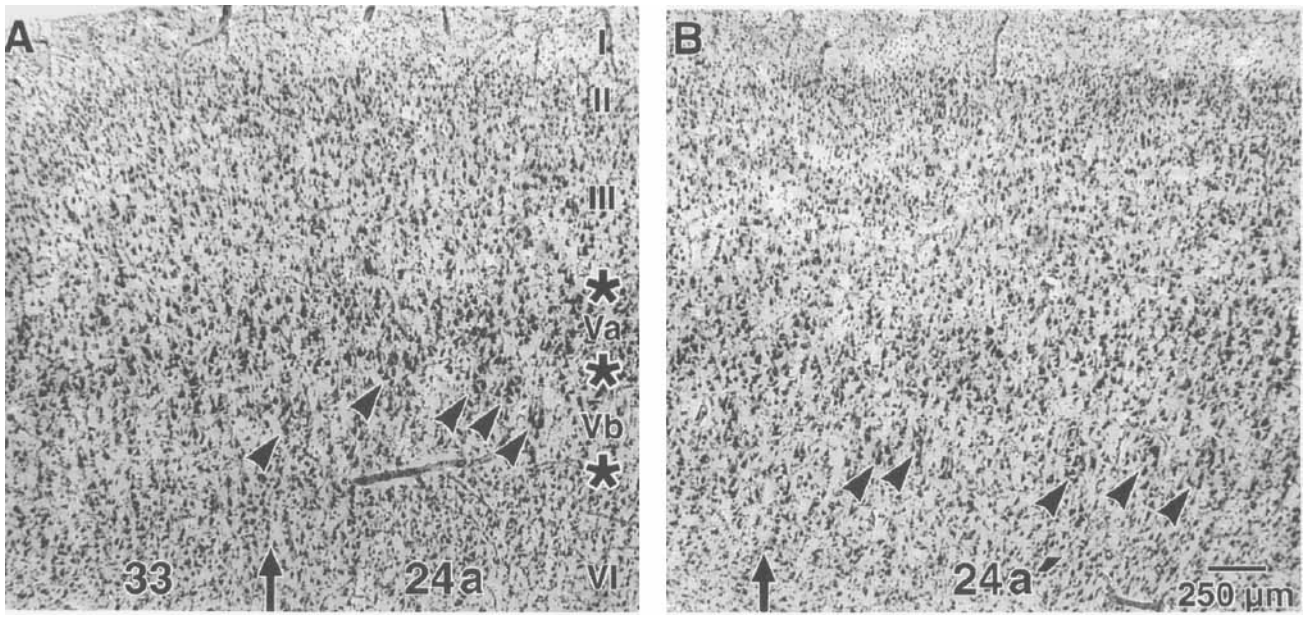

Fig. 6. Area 33/24a (**A**) and 33/24a′ (**B**) junctions (arrows). The asterisks indicate divisions of layer V, and the arrowheads point to clumps of neurons in layer Vb of areas 24a and 24a′.

VI is not clear because layer Vb is poorly formed. Neurons in layer II can form aggregations, as shown in Figure 9, and layer III is composed of homogeneously distributed, medium-sized pyramidal neurons.

Area 24 is an agranular cortex that is characterized by a cell-dense layer Va, and throughout area 24 there is a neuron-sparse layer Vb. Layer Vb is not uniformly devoid of neurons but frequently has clumps of medium to large neurons. These neurons are photographed in subdivisions of area 24, as described below. As is true for von Economo's (1929) anterior cingulate area LA, area 24 has three divisions: a, b, and c. Area 24a lies adjacent to area 33, is in the depths of the callosal sulcus, and extends onto the surface of the cingulate gyrus. Area 24b lies both rostral and dorsal to area 24a, and area 24c lies primarily within the ventral bank of the cingulate sulcus.

Area 24a has definable layers II and III, but the differentiation between these layers is not as pronounced as in more caudal and dorsal areas. This area also has a thin but prominent layer Va, and a layer Vb that is neuron sparse. In layer Vb, however, there are clumps of medium-to-large neurons, as shown in Figure 7. Another cellular feature of area 24a is the high density of spindle pyramidal neurons in layer Vb. Figure 7 shows examples of such neurons. They appear to correspond to neurons originally described by Betz in this region of the human brain and later documented by several authors (Betz, 1881; von Economo, 1926; Ngowyang, 1932; Nimchinsky et al., 1995). These neurons are most prominent in area 24a but are also consistently observed in area 24b, and less frequently in area 24c. They are most numerous in the anterior portion of area 24, and there are instances when such neurons occur in layer Vb of other parts of anterior cingulate cortex including area 32.

Area 24a is not cytoarchitecturally uniform in its rostrocaudal extent. At caudal levels of area 24a (i.e., area 24a′), there is a more clearly defined layer II and a thicker layer III, layer Va is thinner, and layer VI is poorly defined. The area 24 subdivisions are shown in Figure 6. Finally, the clumps of layer Vb pyramidal neurons occur in area 24a′ as well as in area 24a, while the fusiform pyramidal neurons in layer Vb that are characteristic of area 24a are not often observed in area 24a′.

Area 24b lies rostral and dorsal to area 24a. Since transverse sections through area 24b rostral to the genu of the corpus callosum are frequently not perpendicular to the curved cortical surface, blocks from this region were embedded in celloidin and cut into 50- or 100-µm-thick sections at oblique angles so that this region was sectioned perpendicular to area 24b rostral to the corpus callosum; the results of this preparation are shown in Figure 8. Area 24b has the thickest layer Va in the cingulate gyrus. Layer Vb is also broad and contains some typically shaped pyramids as well as many spindle pyramidal neurons. Area 24b has a broad layer III and well-defined layer II with lancet-shaped pyramidal neurons. This area also has been termed anterogenualis magnocellularis by Braak (1979), who noted that the magnocellular region was limited to perigenual cortex.

The cortex on the cingulate gyral surface caudal to area 24b is area 24b′. Area 24b′ has a thinner layer Va, but it is still very prominent and is composed a large pyramidal neurons. Layer Vb has clumps of neurons, as is true for other cingulate areas; one such clump is shown in Figure 7. Frequently when there are aggregations of neurons in layer Vb, the pyramidal neurons in this layer are larger than

Fig. 5. Cytoarchitectural areas superimposed on the flat map of the case in Figure 4. The star is the approximate location of anterior commissure. The shaded lines indicate the brain surface and the apices of each gyrus, and the depths of the sulci are not shown in order to simplify the map. The bold dashed lines outline the cingulate areas, the thinner dashed lines show the borders between each area, and the dotted lines indicate the borders between subdivisions of each area. PaC, paracentral sulcus; CaS, callosal sulcus; CS, cingulate sulcus; Sp, splenial sulcus.

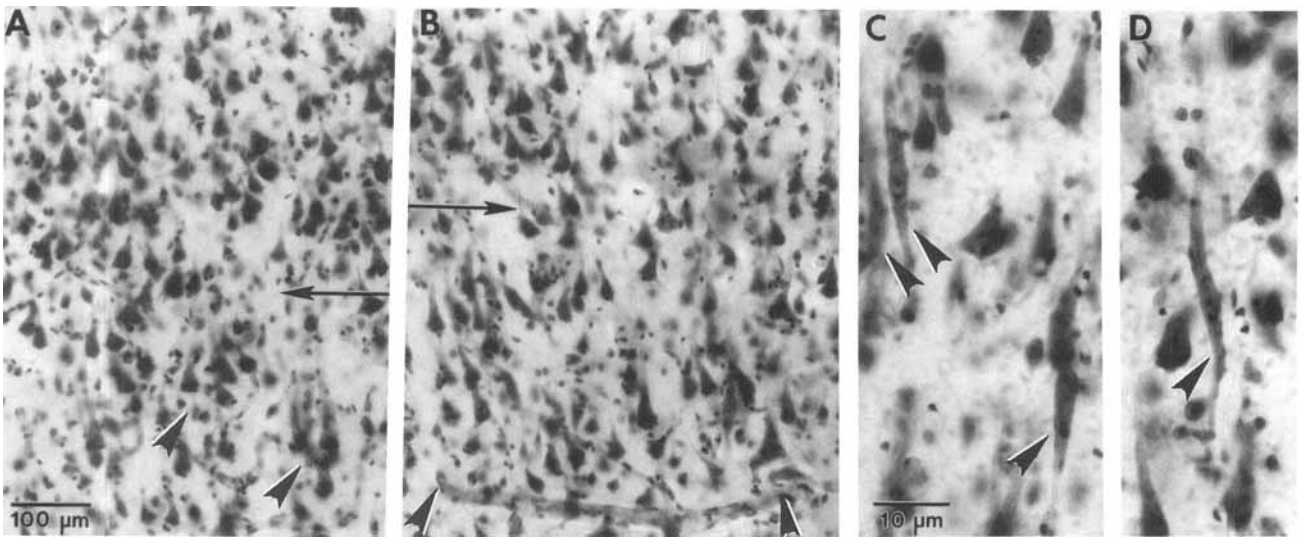

Fig. 7. Aggregations of neurons in layer Vb in area 24a (**A,** arrowheads) and area 24b′ (**B**). The border between layers Va and Vb is indicated with the horizontal arrows. Note in B that the neuronal aggregate in layer Vb is very large and is bounded ventrally by a capillary identified with arrowheads. Neuron-free zones in layer Vb flank each side of this aggregate but are not shown in B. Spindle pyramidal neurons (**C,D,** arrowheads) are characteristic of areas 24a and 24b.

those directly superficial to the clump in layer Va, as in Figure 7. Finally, layer III in area 24b′ is thinner than it is in area 24b.

The ventral bank of the cingulate sulcus contains three cytoarchitectural components of ACC. These are areas 24c, 24c′, and 24c′g, each of which are illustrated in Figure 9. As a general rule the superficial layers II and III of cortex in the depths of the cingulate sulcus are as thick or thicker than layers V and VI. Layer Va is prominent and has more small pyramidal neurons than there are in area 24b, and there are clumps of large neurons in layer Vb. Area 24c lies in the rostral depths of the cingulate sulcus lateral to area 24b. Layer Va is thinner than it is in area 24b, and there are more small pyramids in this layer. The clumps of pyramidal neurons are also more prominent in area 24c because layer Vb is generally more cell sparse. Area 24c′ lies caudal to area 24c and has more medium-sized pyramidal neurons in layer Vb; thus a neuron-free layer is not present. Layer III in area 24c′ is also sparser than it is in area 24c.

Caudal to area 24c′ lies area 24c′g, or the primitive gigantopyramidal area of Braak (1976). As discussed above in terms of the flat map, area 24c′g is usually buried in the depths of the CS. However, in cases with segmented cingulate sulci, the segmentation can occur at a level in which area 24c′g is present; in these instances area 24c′g can extend to the surface of the cingulate gyrus. Layer Va of area 24c′g has more medium-sized than large pyramidal neurons, and layer Vb is characterized by very large pyramidal neurons (Fig. 9). The thickness of this cortex is quite variable. Independent of natural variations around the fundus, some cases have a thick area 24c′, while in other cases it is thin, as in the one shown in Figure 9.

Area 32 is a cingulofrontal transition cortex between area 24 and frontal cortex. Area 32 bounds the rostral and dorsal part of area 24b, is dorsal to areas 24c and 24c′, and terminates near area 24c′g. Area 32 has a clear layer Va that does not reach the thickness and neuron density attained in area 24. The main difference between areas 32 and 24 is the large pyramidal neurons in the deep part of layer III that form a layer IIIc in area 32; these large pyramidal neurons do not occur in area 24. Area 32 is not uniform in its rostrocaudal extent, as can be appreciated in the two photographs of this area in Figure 10. At levels that are rostral and ventral to the genu of the corpus callosum, area 32 is relatively thin and has a dysgranular layer IV. As is true for a number of posterior cingulate areas, layer IV is so thin that large layer IIIc and layer Va pyramidal neurons can intermingle. Layer II is thick and layer IIIa-b is very thin. By contrast, caudal area 32, or area 32′, has an even more attenuated layer IV, layer IIIc pyramidal neurons are larger, and layer Va is not nearly as dense as it is at rostral levels of area 32.

Cytoarchitecture of posterior cingulate cortex

Posterior cingulate cortex is characterized by granular layers II and IV. The periallocortical areas 29 and 30 have a poorly differentiated external pyramidal layer, while isocortical area 23 has a thick layer IV and well-defined layers II, IIIa-b, and IIIc. As the CS arches to form the marginal ramus, it no longer delineates cingulate cortex but becomes buried in the medial parietal cortex. At caudal levels of the cingulate gyrus the splenial sulcus usually delineates cingulate area 23 from cinguloparietal transition area 31.

Area 29 has two divisions. There is a lateral division (area 291) that is cell-dense and poorly differentiated. In this instance there are only two layers, a dense and granular external pyramidal layer and a layer V. The medial division of area 29 (area 29m) has layers III and IV of the external layers, layer V is clearly divisible into layer Va of large neurons and a sparse layer Vb, and there is a thin layer VI.

Area 30 is a proisocortical area with a dysgranular layer IV. A dysgranular layer IV is thin and of variable thickness, and at points the large pyramidal neurons in layers IIIc and Va can actually merge. The architecture of area 30 is shown in Figure 11. Layers II–IIIa-b are poorly differentiated and layer IIIc has large pyramidal neurons; some of these are in layer IV, as marked in Figure 11.

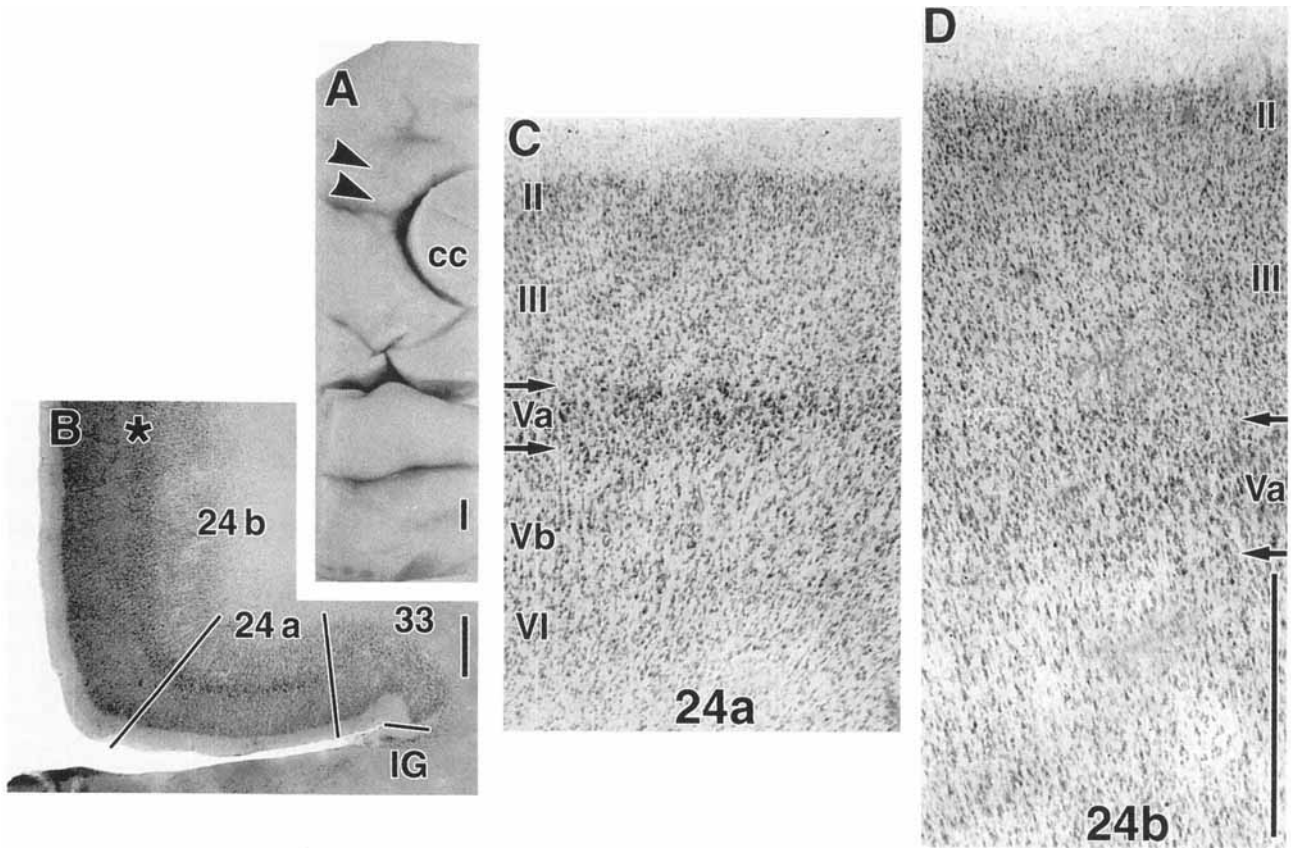

Fig. 8. Perigenual region in a case (man, 61 years old) from which blocks were removed for sectioning perpendicular to the anterogenual cortex. **A:** The top arrowhead is the plane of section for block two of three blocks, while the second arrowhead is the level of the macrophotograph in B. **B:** The asterisk designates layer Va and IG is indusium griseum. **C:** Higher magnification of area 24a with layer Va marked by arrows. **D:** Higher magnification of area 24b with layer Va also marked with arrows for comparison to that in area 24a. Celloidin, 100-μm-thick section. Scale bars = 1 mm.

Area 23 is characterized by well-differentiated layers IIIc, IV, and Va; however, it is not uniform in its ventral-to-dorsal extent. The cytoarchitectural patterns of its three divisions are shown in Figure 11. Area 23a is adjacent to area 30 and has prominent layers IIIc and IV. Although it has a layer Va, the pyramidal neurons in this layer tend to be small and difficult to detect at low magnifications. Area 23b lies dorsal to area 23a and forms much of the posterior cingulate gyral surface. Area 23b has many features that are similar to area 23a, including well-developed layer IIIc pyramids and a thick layer IV. Area 23b, however, has a pronounced layer Va and large pyramidal neurons throughout layer V (Fig. 11). Area 23c is located in the depths of the CS dorsal to the rostral part of area 23b. Area 23c has broad layers II–III, and layer III is more differentiated in this area than it is in any other cingulate area. Thus, there are progressively larger pyramidal neurons in layers IIIa, IIIb, and IIIc. In comparison to area 23b, the large pyramids in layer IIIc are sparse and smaller. Area 23c has a thin layer IV that is dysgranular and it often appears that layer Va is somewhat granular because of the many small neurons in this layer. Further confounding the border between layers IV and Va are the presence of large pyramidal neurons in layer IV (Fig. 11, arrowheads). In comparison to other parts of area 23, layers V and VI are compressed, and layer V is poorly differentiated. Layer VI is thinner than in any other cingulate area. Thus, area 23c has a much larger proportion of its thickness composed of layers I–IV than is true for areas 23a and 23b, and the differentiation between layers IV and Va is not pronounced.

The parasplenial lobules are between a superior branch of the Sp and a caudal branch of the CS and between the Sp and the PO (stars in Fig. 2). It is in this region that Brodmann defined area 31 and it is in the parasplenial lobule that area 31 is photographed in Figure 10. In comparison to area 23c, area 31 has a very broad layer IIIc with larger pyramidal neurons than in layer IIIc of any other cingulate area. Layer IIIa-b in area 31 is quite narrow, while layer IV is very thick and much broader than in either area 23b or area 23c. The vertical orientation of neurons in area 31 is particularly pronounced in layers III and IV of area 31 when compared with that of other cingulate areas (Schlaug et al., 1995) and emphasizes its transitional character with medial parietal cortex. Finally, area 31 has a prominent layer V of large pyramidal neurons, a layer Vb of sparse pyramidal neurons is not usually detectable, and there is a well-defined layer VI of small neurons.

Cytoarchitectural variability in area 23

The above description of cingulate cortex cytoarchitecture is a generalization from observations of common area

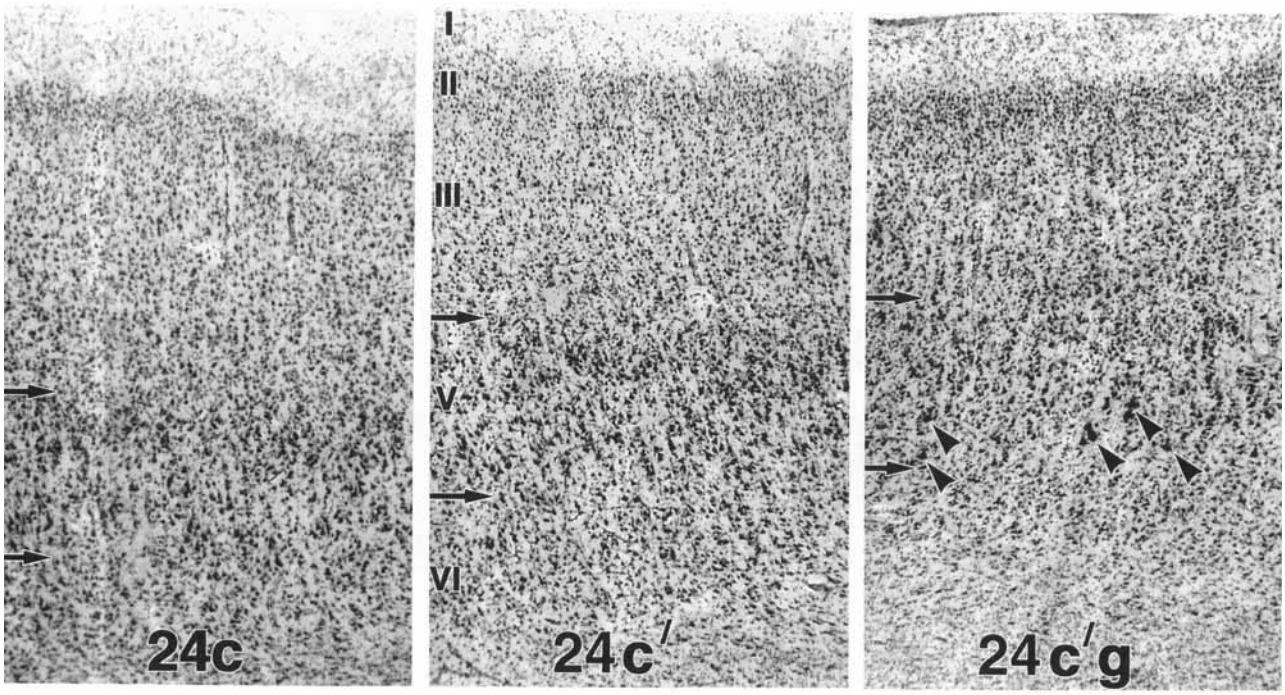

Fig. 9. Cingulate sulcal region of area 24 at progressively more caudal levels (man, 62 years old). Layer V is delineated for each area with arrows at its superficial and deep borders. In area 24c'g the gigantopyramidal neurons in layer Vb are indicated with arrowheads. Celloidin, 60-μm-thick sections.

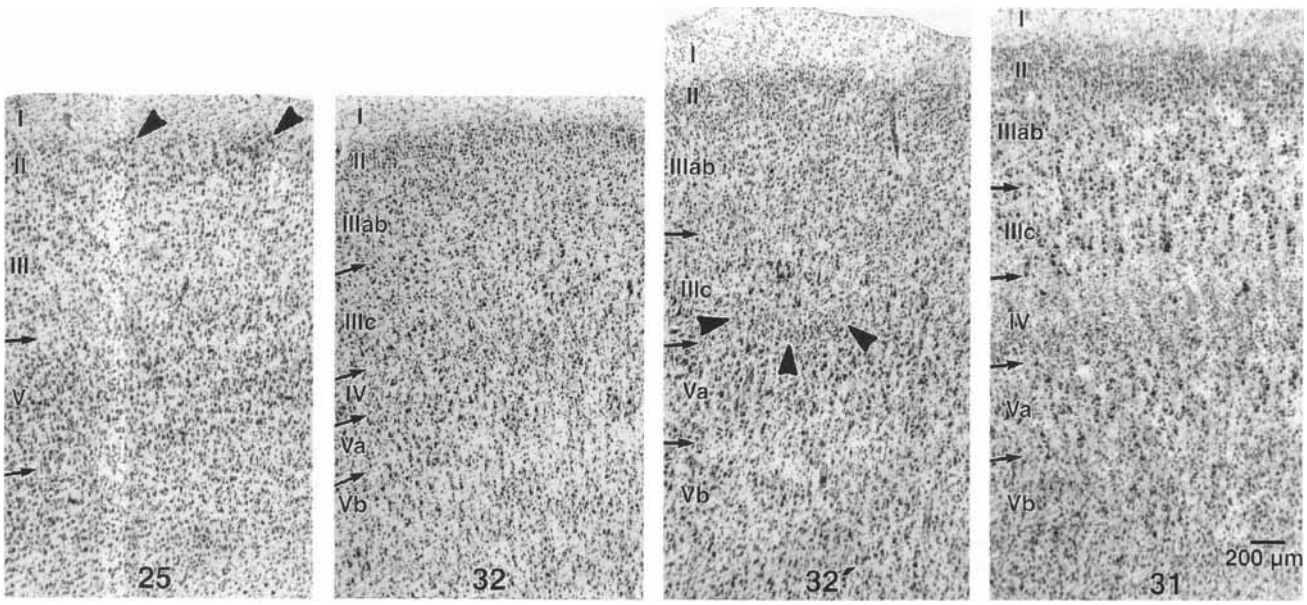

Fig. 10. Area 25 and the cingulate transition areas 32 and 31. Area 25 has neuronal aggregates in layer II (arrowheads), whereas layer II is slender and uniform in the other areas. Layer IV is dysgranular in area 32, and in area 32' the large layer IIIc and layer Va pyramids can intermingle. (There is only a thin layer IV, designated here with three arrowheads.) Celloidin; area 25 is 35-μm-thick section from 74-year-old man, and all others are 50 μm thick and are from a 45-year-old woman.

features in 11 cases. In order to assess the extent to which the architecture of a single area may vary among individuals, the density of neurons in each layer of a parasplenial level of area 23a was assessed in 13 cases. This parasplenial level of area 23 was chosen because it can be consistently identified in all cases and ensures a constant sampling region. The mean ± SEM number of neurons in each layer was as follows: II, 59 ± 4.2; IIIa/b, 66 ± 6.2; IIIc, 56 ± 2.9; IV, 54 ± 5.9; Va, 53 ± 2.8; Vb, 36 ± 2.3; and VI, 82 ± 9.5. Since it has been reported that the density of large neurons decreases with age (Terry et al., 1987), we assessed the relationships between age (range, 45–102 years) and neu-

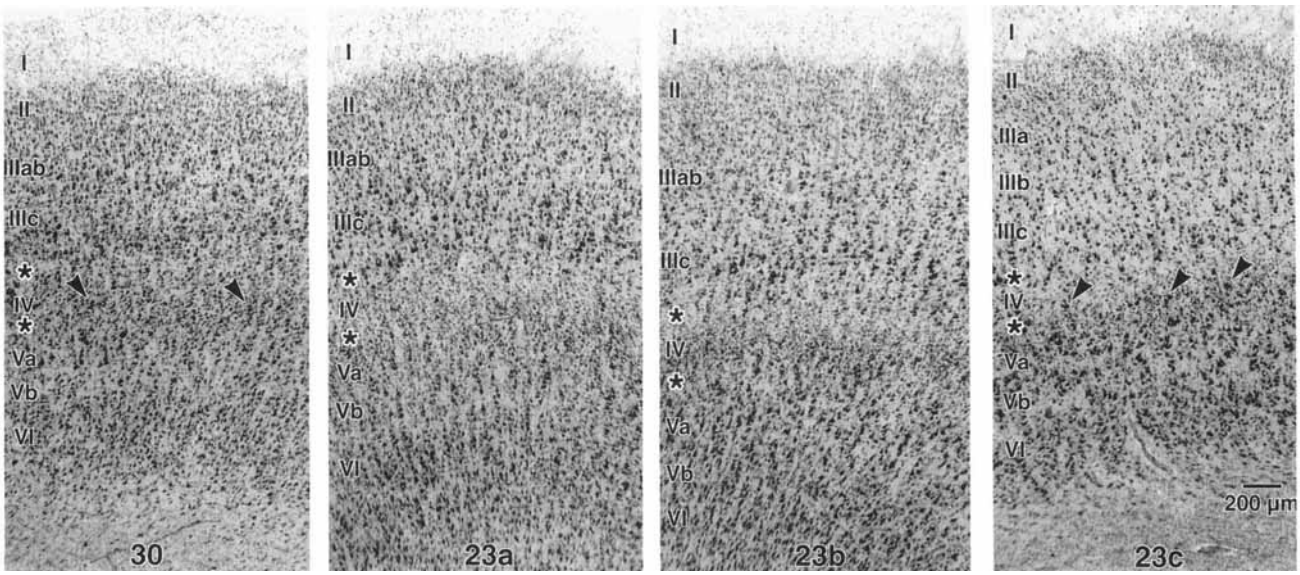

Fig. 11. Areas in PCC (woman, 45 years old). Both areas 30 and 23c are dysgranular. There are occasional large pyramidal neurons in layer IV (arrowheads), and the large neurons in layers IIIc and Va can be closely apposed. The superficial and deep borders of layer IV are shown with asterisks. Celloidin, 50-µm-thick sections.

ron density in each layer of area 23a. The correlation coefficient of −0.63 was significant ($P = 0.046$) for layer IV, whereas correlations for remaining layers were not significant. It was interesting to note that the other layer of small neurons (i.e., layer II) had a correlation of −0.41, whereas layers with the largest neurons had very weak correlations (i.e., layer IIIc, r = −0.02 and layer Va, r = −0.20). Figure 12 shows examples of strips of neuronal perikarya through layers IIIc–Va in which the decline in neuron density in layer IV is apparent. Although there is a pronounced decline in neuron density in layer IV, and possibly some shrinkage in large neurons, over the period of six decades, these changes do not alter the relative organization of layers of PCC and the laminar architecture can still be identified. Additionally, it is possible that neurons in layers IIIc and Va shrink throughout this time, although this parameter was not quantified in the present study.

DISCUSSION

The present assessment of cingulate cortex expands upon the original Brodmann (1909) and Retzius (1896) accounts of the human brain in the following ways: 1) the variation of medial surface features are detailed and include a flexible nomenclature and definition of the parasplenial lobules; 2) the cytoarchitectural differentiation encountered within each region of cingulate cortex is presented (i.e., differences among the a, b, and c subdivisions of areas 24 and 23); 3) the sulcal areas including the motor fields are characterized and their topography defined on a flattened medial cortical surface; 4) cytoarchitectural differences in the rostral and caudal parts of area 24 are defined (i.e., those between areas 24 and 24′); 5) interindividual variation in laminar cytoarchitecture is quantified for area 23; and 6) the features of the cingulofrontal transition areas 32 and 32′ and cinguloparietal transition area 31 are specified.

Studies of neurons in primate cingulate cortex that are immunoreactive for nonphosphorylated neurofilament protein have shown that variations in their distribution correspond with the cytoarchitectonic fields described in the present report (Hof and Nimchinsky, 1992; Vogt et al., 1992). In human, ACC is distinguishable from PCC by the general paucity of neurofilament protein-immunoreactive neurons, and the near absence of these cells in layer III. The spindle pyramidal neurons of layer Vb that are most dense in areas 24a and 24b are strongly neurofilament protein-immunoreactive (Nimshinsky et al., 1995). The region corresponding to area 24c′g is distinguished by very large, intensely immunoreactive pyramidal neurons in layer V and numerous, somewhat smaller pyramidal neurons in layer III. Area 25 resembles area 24a in that it contains a few neurofilament protein-positive neurons that are restricted to layer V. An area of transition abutting area 24′ is evident between anterior and posterior cingulate cortex in all the subfields and displays a progressive increase in the density of neurofilament protein-immunoreactive neurons in layer III. The PCC contains large numbers of neurofilament protein-containing neurons in both supra- and infragranular layers, with the greatest density in layer III of area 23c. In the callosal sulcus, area 291 contains small immunoreactive pyramidal neurons in layer V, and area 29m is distinguishable as the region where immunoreactive neurons appear, sporadically in the more lateral portion, and then medially with greater density in layer III.

In a recent assessment of the rabbit and monkey cingulate cortices (Vogt, 1993), area 24 was divided into rostral area 24 and caudal area 24′. This was done to account for cytoarchitectural and connection differences between these parts of area 24. Area 24 in these experimental animals has a cell-dense layer V and receives substantial input from the amygdala and limited inputs from parietal cortex. By contrast, area 24′ has denser neurons in layer Va, receives

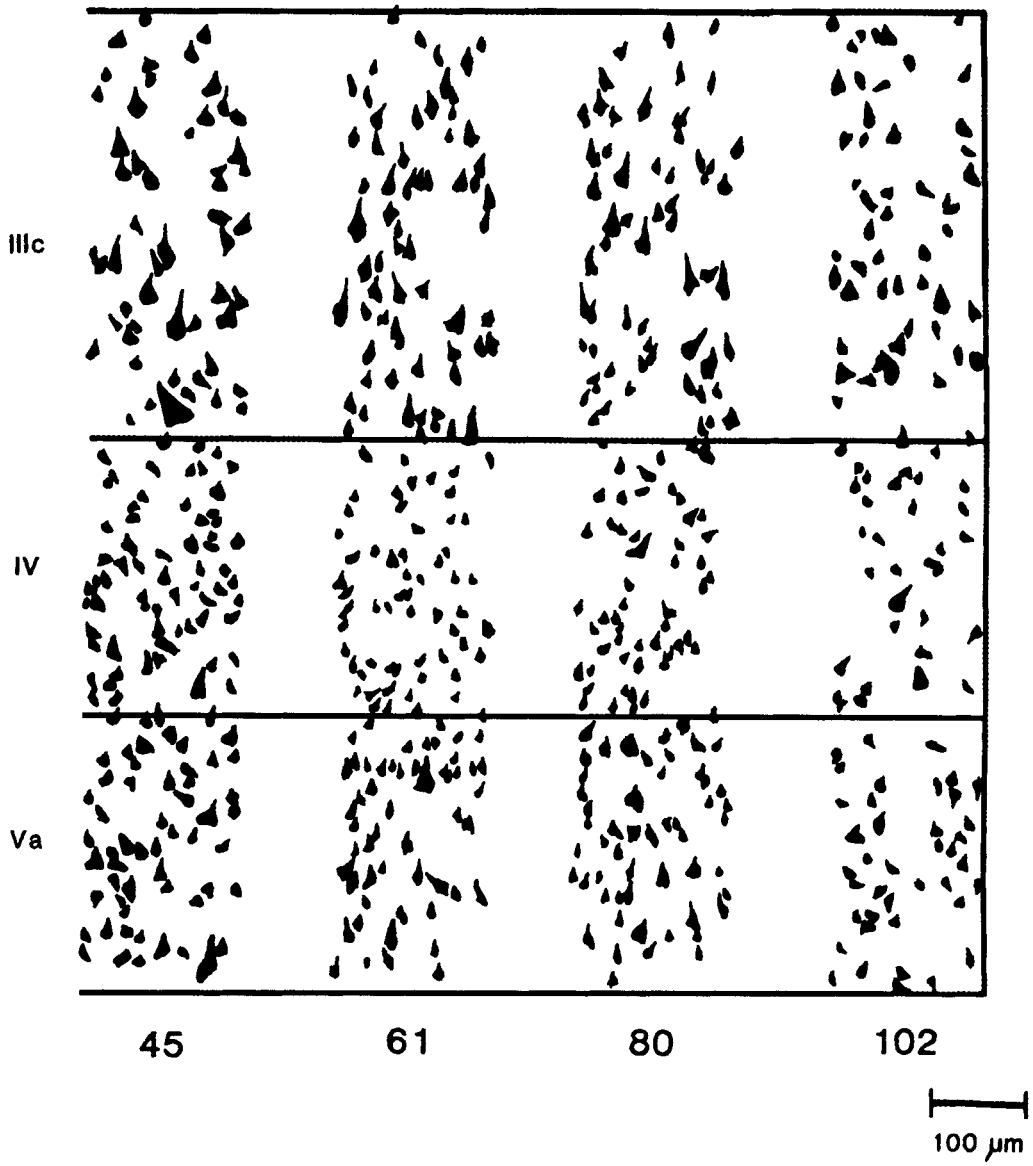

Fig. 12. Neuronal perikaya in mid-cortical layers of area 23a in four cases with the age shown below each.

little amygdala input, and has a larger component of parietal lobe afferents. This concept has been extended to the human brain because of the prominent cytoarchitectural differences between the anterior and posterior parts of area 24. Braak (1979) described an anterogenual magnocellular area in rostral area 24, and this area is included in rostral area 24b of the present assessment. In terms of comparing the human and monkey cingulate cortices, it appears that area 24′ in the monkey has both denser and larger pyramidal neurons than is the case for area 24. By contrast, human area 24 has a broader and denser layer Va, and it is in area 24′ that the neurons are larger in this layer, which does not reach the same neuron density and laminar thickness as in area 24. Finally, the anterogenual field of Braak does not appear to include area 32 because area 32 has prominent layer IIIc pyramidal neurons that are not characteristic of area 24.

A comparison of the present cytoarchitectural map for humans and a previous one for the rhesus monkey (Vogt, 1993) provides a basis for comparisons of the composition of cingulate cortex in these species. The following parts of cingulate cortex are larger in the human brain: 1) cortical surface in the callosal sulcus in anterior cortex, which includes area 33; 2) area 24′ is longer in the rostrocaudal orientation and includes area 24c′g; 3) there is an extensive region of cingulofrontal transition cortex where area 32′ forms a dorsal border for areas 24 and 24′; and 4) the cinguloparietal transition cortex is so large that it is thrown into folds, termed the parasplenial lobules, which are not present in monkey cortex. Comparative studies of PCC using quantitative, volumetric techniques provide important advances for detailing structural differences among species (Armstrong et al., 1986; Zilles et al., 1986). Thus, it is now possible to characterize the structural differences

between primate species in ACC and PCC at a new level of detail, and such studies should provide insight into the functional organization of cingulate cortex.

Terry et al. (1987) showed a reduction in large neuron densities in midfrontal, superior temporal, and inferior parietal cortices over a wide range of ages (24–100 years), whereas no changes were observed in small neuron densities. Since this analysis did not consider neuron densities by layer, it is possible that laminar-specific changes, such as those observed in the present study in layer IV and those in layers III and V (Mann et al, 1985), were not observed. It is also possible that neurons shrink throughout the course of aging, as is suggested qualitatively in Figure 12, such that some neurons that may have been documented as large neurons early in life are considered small neurons later in life. Although the present study did not include individuals below the age of 45, the present findings suggest that PCC may undergo processes that are unique in the cerebral cortex. It appears that, although the large neurons in this region may shrink, they remain relatively constant in number and may be selectively protected against damage to which neurons succumb in other neocortical areas. Nonetheless, the function of PCC could be critically disrupted as a consequence of aging processes due to the loss of small pyramidal neurons in layer IV.

One of the most important findings in recent architectural studies of cingulate cortex is the presence of the cingulate motor areas. Braak (1976) first identified a primitive gigantopyramidal area in the depths of the cingulate sulcus that was not continuous with primary motor cortex. Parts of this region in the monkey project to the spinal cord (Biber et al., 1978), and these projections have been used to define three cingulate motor areas (Dum and Strick, 1991, 1993). It appears that a rostral cingulate motor area is in area 24c′ and a ventral cingulate motor area is in area 23c, whereas a third area is in the dorsal bank of the CS. The extent to which the caudal part of area 24c′ in monkey is homologous to area 24c′g in the human is not presently known. Finally, there is evidence for premotor function for these areas in monkey. Shima et al. (1991) demonstrated that single neurons in the depths of the CS discharged long before movement execution. In addition, electrical stimulation in this region evokes skeletomotor responses from somatotopically organized motor fields (Luppino et al., 1991).

The ACC has many projections to brainstem motor systems including the caudate, pontine, and red nuclei as well as cortical premotor areas (reviewed by Van Hoesen et al., 1993). Most of these projections, including those from the spinal cord, originate from layer V. Layer V in area 24 is also characterized by pyramidal neurons with more extensive dendritic arbors than those in area 23 (Schlaug et al., 1993). Another feature of human area 24 noted in the present work is the clumping of pyramidal neurons in layer Vb. It is possible that these clumps of neurons are engaged as a functional unit and that they project to brainstem motor structures. Furthermore, in ACC of young rhesus monkeys there are clumps of neurons in layer Vb that are immunoreactive for dopamine and cyclic adenosine monophosphate (cAMP)-regulated phosphoprotein-32 (DARPP-32; Berger et al., 1990, see their Fig. 29), and these neurons express high levels of dopamine D1 receptors. Since layer V is the defining feature of area 24, the architecture and circuitry of area 24 should be evaluated further for clues into its role in premotor function.

The cingulofrontal transition area 32 has a significantly wider topographical distribution in the human brain than it does in nonhuman primates. In the rhesus monkey, for example, area 32 has a thin layer IV and is located rostral to area 24 (Vogt et al., 1987). In the human, by contrast, Brodmann (1909) suggested that it extends around the rostral and dorsal border of area 24, and this was confirmed in the present cases. Although area 32 is characterized by large layer IIIc pyramidal neurons, it is not uniform throughout its rostrocaudal extent, and so the Brodmann nomenclature was further modified. Rostral area 32 has a well-defined layer Va and a dysgranular layer IV. Caudal area 32′ has virtually no layer IV, very large layer IIIc pyramidal neurons, and a much less prominent layer Va. von Economo (1929) carried the concept of area 32 differentiation (L for limbic in his nomenclature) even further. He proposed that there are at least four divisions of cingulofrontal transition cortex in relationship to the adjoining frontal cortical areas. It is possible, therefore, that area 32 may be divided even further to account for subtle gradations in cytoarchitecture.

There is limited evidence as to the function of the cingulofrontal transition areas 32 and 32′. Blood flow has been elevated in this area in a word generation task by Raichle et al. (1994). In this study the subject was scanned while generating verbs to a list of nouns. With practice the elevated blood flow in what appears to be part of area 32′ was reduced to baseline values, and a novel list of nouns reactivated a similar region. Grasby et al. (1993) also showed that this area is likely involved in declarative memory processes. Thus, area 32′ appears to be involved in response selection for unrehearsed behaviors, and this requires mechanisms for memory access. Finally, area 32 is involved in functions associated with emotion including assessing pictures of faces with affective content (George et al., 1995). This is compatible with previously proposed anatomical and functional observations that rostral parts of ACC are engaged in affect, while posterior and dorsal parts are involved in cognition (Devinsky et al., 1995). The role of areas 32 and 32′ in the initiation of behaviors that involve affect is underscored by findings of Bench et al. (1992) that it is probably inactivated in cases of major depression.

The direct application of cytoarchitectural analyses to human brain imaging problems is an important area of current research, and the Talairach and Tournoux (1988) atlas is frequently used for functional studies. A number of inaccuracies in this atlas, however, have led to confusion in specifying regions of functionally activated cortex on the medial surface. In a medial view (Talairach and Tournoux, 1988, their Fig. 9), area 32 is shown flanking the CS, whereas area 24 is ventral to parallel dimples in the cingulate gyrus. This interpretation differs from the original description of Brodmann (1909) and their own interpretation of the coronal sections presented later in the atlas. Furthermore, the cingulate sulcus is termed the "sulcus callosomarginalis" (Talairach and Tournoux, 1988, their Fig. 13), whereas in transverse sections the CS is not labeled. Careful definition of the CS in medial surface reconstructions from magnetic resonance (MR) images will allow for determination of whether area 32 and/or area 24 are activated in functional imaging studies. Finally, areas 29 and 30 are incorrectly shown as being exposed on the gyral surface at the level of the caudomedial lobule in PCC. This is likely a misinterpretation based on Brodmann's attempt to display these areas in the depths of the callosal

sulcus on a convoluted brain surface that was not extended into a flat map format.

The junction of PCC with the parietal lobe is occupied by area 31. Brodmann extended area 31 into the CS but did not identify an area 23c in this region as we have done previously in the rhesus monkey (Vogt et al., 1987). We continue the use of area 23c in the caudal depths of the human CS for cytoarchitectural reasons and because the cingulate motor area in area 23c does not extend onto the gyral surface to include area 31. Although the unique contributions of the cinguloparietal transition area 31 to primate behavior are not known, it may be engaged with areas 23a and 23b in visuospatial orientation. Neurons in this region code for the position of the eye in the orbit following eye movements, they respond to large textured stimuli, and they are influenced by background illumination (Olson et al., 1993). Lesions in PCC impair spatial delayed non-matching to sample behavior in monkeys (Murray et al., 1989). As concluded by Olson et al. (1993), posterior cingulate neurons may "utilize oculomotor signals in the service of visual information processing." In this context it is interesting that individuals with Alzheimer's disease with a prominent and complex visual symptomatology referred to as Balint's syndrome have high densities of neurofibrillary tangles in PCC (Hof et al., 1990, 1993).

The first generation of functional imaging studies during the 1980s made important contributions to understanding the role of the medial cortex in human behavior and information processing in the brain. The specific areas activated were difficult to identify, however, without coregistration of PET and MR images. Future functional imaging research will emphasize such coregistration as well as functional MR to provide a higher resolution of the particular areas thus activated. In the context of the present and other cytoarchitectural studies, functional imaging of the brain can be used to determine specifically which rostrocaudal and dorsoventral parts of cingulate cortex are activated so that a clearer estimation can be made of the area(s) involved. This added level of structural detail will provide a better understanding of the mechanisms of cortical information processing in the human brain and specific hypotheses to direct mechanistic studies in nonhuman primates.

ACKNOWLEDGMENTS

We thank the following individuals for providing us with postmortem cingulate cortices: Dr. Gary W. Van Hoesen and Loren Spence, Department of Anatomy, University of Iowa, Iowa City, IA; Dr. Deepak N. Pandya, Veterans Administration Hospital, Bedford, MA; Dr. Constantin Bouras, Department of Psychiatry, University of Geneva, Geneva, Switzerland; and Dr. Daniel P. Perl, Division of Neuropathology, Mount Sinai School of Medicine, New York, NY. We also thank Beverly McClellan for help in preparing Figure 5.

This research was supported by NIH-NIA grants AG11480 and AG05138, the Brookdale Foundation, and the Bowman Gray School of Medicine Brain/DNA Resource Center.

LITERATURE CITED

Armstrong, E., K. Zilles, G. Schlaug, and A. Schleicher (1986) Comparative aspects of the primate posterior cingulate cortex. J. Comp. Neurol. *253:*539–548.

Bates, J.F., and P.S. Goldman-Rakic (1993) Prefrontal connections of medial motor areas in the rhesus monkey. J. Comp. Neurol. *335:*1–18.

Bench, C.J., K.J. Friston, R.G. Brown, L.C. Scott, R.S.J. Frackowiak, and R.J. Dolan (1992) The anatomy of melancholia—focal abnormalities of cerebral blood flow in major depression. Psychol. Med. *22:*607–615.

Berger, B., A. Febvret, P. Greengard, and P.S. Goldman-Rakic (1990) DARPP-32, a phosphoprotein enriched in dopaminoceptive neurons bearing dopamine D1 receptors: Distribution in the cerebral cortex of the newborn and adult rhesus monkey. J. Comp. Neurol. *299:*327–348.

Betz, W. (1881) Uber die feinere Structur der Gehirnrinde des Menschen. Zentralbl. Med. Wiss. *19:*193–195, 209–213, 231–234.

Biber, M.P., L.W. Kneisley, and J.H. LaVail (1978) Cortical neurons projecting to the cervical and lumbar enlargements of the spinal cord in young adult rhesus monkeys. Exp. Neurol. *59:*492–508.

Braak, H. (1976) A primitive gigantopyramidal field buried in the depth of the cingulate sulcus of the human brain. Brain. Res. *109:*219–233.

Braak, H. (1979) Pigment architecture of the human telencephalic cortex V. Regio anterogenualis. Cell Tissue Res. *204:*441–451.

Brodmann, K. (1909) Vergleichende Lokalisationslehre der Gro$hirnrinde in ihren Prinzipien dargestellt auf Grund des Zellenbaues. Liepzig: Barth.

Casey, K.L., S. Minoshima, K.L. Berger, R.A. Koeppe, T.J. Morrow, and K.A. Frey (1994) Positron emission tomographic analysis of cerebral structures activated specifically by repetitive noxious heat stimuli. J. Neurophysiol. *71:*802–807.

Corbetta, M., F.M. Meizir, S. Dobmeyer, G.L. Shulman, and S.E. Petersen (1991) Selective and divided attention during visual discrimination of shape, color, and speed: Functional anatomy by positron emission tomography. J. Neurosci. *11:*2383–2402.

Devinsky, O., M.J. Morrell, and B.A. Vogt (1995) Contributions of anterior cingulate cortex to behavior. Brain *118:*279–306.

Dum, R.P., and P.L. Strick (1991) The origin of corticospinal projections from the premotor areas in the frontal lobe. J. Neurosci. *11:*667–689.

Dum, R.P., and P.L. Strick (1993) The cingulate motor areas. In B.A. Vogt and M. Gabriel (eds): Neurobiology of Cingulate Cortex and Limbic Thalamus. Boston: Birkhäuser, pp. 415–441.

George, M.S., T.A. Ketter, D.S. Gill, J.V. Haxby, L.G. Ungerleider, P. Herscovitch, and R.M. Post (1993) Brain regions involved in recognizing facial emotion or identity: An oxygen-15 PET study. J. Neuropsychol. Clin. Neurosci. *5:*384–394.

George, M.S., T.A. Ketter, P.I. Parekh, B. Horowitz, P. Herscovitch, and R.M. Post (1995) Brain activity during transient sadness and happiness in healthy women. Am. J. Psychiatry *153:*341–351.

Grasby, P.M., C.D. Frith, K.J. Friston, C. Bench, R.S.J. Frackowiak, and R.J. Dolan (1993) Functional mapping of brain areas implicated in auditory-verbal memory function. Brain *116:*1–20.

Hof, P.R., and E.A. Nimchinsky (1992) Regional distribution of neurofilament and calcium-binding proteins in the cingulate cortex of the macaque monkey. Cerebral Cortex *2:*456–467.

Hof, P.R., C. Bouras, J. Constantinidis, and J.H. Morrisson (1990) Selective disconnection of specific association pathways in cases of Alzheimer's disease presenting with Balint's syndrome. J. Neuropathol. Exp. Neurol. *49:*168–184.

Hof, P.R., N. Archin, A.P. Osmand, J.H. Dougherty, C. Wells, C. Bouras, and J.H. Morrison (1993) Posterior cortical atrophy in Alzheimer's disease: Analysis of a new case and re-evaluation of a historical report. Acta Neuropathol. *86:*215–223.

Jones, A.K.P., W.D. Brown, K.J. Friston, L.Y. Qi, and R.S.J. Frackowiak (1991) Cortical and subcortical localization of response to pain in man using positron emission tomography. Proc. R. Soc. Lond. [Biol.] *244:*39–44.

Luppino, G., M. Matelli, R.M. Camarda, V. Gallese, and G. Rizzolatti (1991) Multiple representations of body movements in mesial area 6 and the adjacent cingulate cortex: An intracortical microstimulation study in the macaque monkey. J. Comp. Neurol. *311:*463–482.

Mann, D.M.A., P.O. Yates, and B. Marcyniuk (1985) Some morphometric observations on the cerebral cortex and hippocampus in presenile Alzheimer's disease, senile dementia of Alzheimer type and Down's syndrome in middle age. J. Neurol. Sci. *69:*139–159.

Matelli, M., G. Luppino, and G. Rizzolatti (1991) Architecture of superior and mesial area 6 and the adjacent cingulate cortex in the macaque monkey. J. Comp. Neurol. *311:*445–462.

Morecraft, R.J., and G.W. Van Hoesen (1992) Cingulate input to the primary and supplementary motor cortices in the rhesus monkey: Evidence for somatotopy in cingulate areas 24c and 23c. J. Comp. Neurol. *322:*471–489.

Murray, E.A., M. Davidson, D. Gaffan, D.S. Olton, and S. Suomi (1989) Effects of fornix transection and cingulate cortical ablation on spatial memory in rhesus monkeys. Exp. Brain Res. *74:*173–186.

Ngowyang, G. (1932) Beschreibung einer Art von Spezialzellen in der Inselrinde: zugleich Bemerkungen über die v. Economoschen Spezialzellen. J. Psychol. Neurol. *44:*671–674.

Nimchinsky, E.A., B.A. Vogt, J.H. Morrison, and P.R. Hof (1995) Spindle neurons in the human cingulate cortex: A histochemical analysis. J. Comp. Neurol. *355:*27–37.

Olson, C.R., S.Y. Musil, and M.E. Goldberg (1993) Posterior cingulate cortex and visuospatial cognition: Properties of single neurons in the behaving monkey. In B.A. Vogt and M. Gabriel (eds): Neurobiology of Cingulate Cortex and Limbic Thalamus. Boston: Birkhäuser, pp. 366–380.

Ono, M., S. Kubik, and C.D. Abernathey (1990) Atlas of the Cerebral Sulci. New York: Georg Thieme Verlag.

Pardo, J.V., P.J. Pardo, K.W. Janer, and M.E. Raichle (1990) The anterior cingulate cortex mediates processing selection in the Stroop attentional conflict paradigm. Proc. Natl. Acad. Sci. USA *87:*256–259.

Petersen, S.E., P.T. Fox, M.I. Posner, M. Mintum, and M.E. Raichle (1988) Positron emission tomographic studies of the cortical anatomy of single word processing. Nature *331:*585–589.

Petit, L., C. Orssaud, N. Tzourio, G. Salamon, B. Mazoyer, and A. Berthoz (1993) PET study of voluntary saccadic eye movements in humans: Basal ganglia-thalamocortical system and cingulate cortex involvement. J. Neurophysiol. *69:*1009–1017.

Raichle, M.A., J.A. Fiez, T.O. Videen, A.-M.K. MacLeod, J.V. Pardo, P.T. Fox, and S.E. Petersen (1994) Practice-related changes in human brain functional anatomy during nonmotor learning. Cerebral Cortex *4:*8–26.

Retzius, G. (1896) Das Menschenhirn. Studien in der makroskopischen Morphologie. Stockholm: Norstedt.

Schlaug, G., E. Armstrong, A. Schleicher, and K. Zilles (1993) Layer V pyramidal cells in the adult human cingulate cortex. Anat. Embryol. *187:*515–522.

Schlaug, G., U. Knorr, and R.J. Seitz (1994) Inter-subject variability of cerebral activations in acquiring a motor skill: A study with positron emission tomography. Exp. Brain Res. *98:*523–534.

Schlaug, G., A. Schleicher, and K. Zilles (1995) Quantitative analysis of the columnar arrangement of neurons in the human cingulate cortex. J. Comp. Neurol. *351:*441–452.

Shima, K., K. Aya, H. Mushiake, M. Inase, and J. Tanji (1991) Two movement-related foci in the primate cingulate cortex observed in signal-triggered and self-paced forelimb movements. J. Neurophysiol. *65:*188–202.

Talairach, J. and P. Tournoux (1988) Co-Planar Stereotaxic Atlas of the Human Brain. New York: Thieme Medical Publishers.

Talbot, J.D., S. Marrett, A.C. Evans, E. Meyer, M.C. Bushnell, and G.H. Duncan (1991) Multiple representations of pain in human cerebral cortex. Science *251:*1355–1358.

Terry, R.D., R. DeTeresa, and L.A. Hansen (1987) Neocortical cell counts in normal human adult aging. Ann. Neurol. *21:*530–539.

Van Hoesen, G.W., R.J. Morecraft, and B.A. Vogt (1993) Connections of the monkey cingulate cortex. In B.A. Vogt and M. Gabriel (eds): Neurobiology of Cingulate Cortex and Limbic Thalamus. Boston: Birkhäuser, pp. 249–284.

Vogt, B.A. (1976) Retrosplenial cortex in the rhesus monkey: A cytoarchitectonic and Golgi study. J. Comp. Neurol. *169:*63–98.

Vogt, B.A. (1993) Structural organization of cingulate cortex: Areas, neurons, and somatodendritic transmitter receptors. In B.A. Vogt and M. Gabriel (eds): Neurobiology of Cingulate Cortex and Limbic Thalamus. Boston: Birkhäuser, pp. 19–70.

Vogt, B.A., D.N. Pandya, and D.L. Rosene (1987) Cingulate cortex of the rhesus monkey: I. Cytoarchitecture and thalamic afferents. J. Comp. Neurol. *262:*256–270.

Vogt, B.A., E.A. Nimchinsky, P.R. Hof, and J.H. Morrison (1992) Chemoarchitecture of the monkey and human cingulate cortex. Soc. Neurosci. Abs. *18:*1419.

Vogt, C., and O. Vogt (1919) Allgemeinere Ergebnisse unserer Hirnforschung. J. Psychol. Neurol. (Leipzig) *25:*277–462.

von Economo, C. (1926) Eine neue Art Spezialzellen des Lobus cinguli und Lobus insulae. Z. Ges. Neurol. Psychiatr. *100:*706–712.

von Economo, C. (1929) The Cytoarchitectonics of the Human Cerebral Cortex. London: Oxford University Press.

Zilles, K., E. Armstrong, G. Schlaug, and A. Schleicher (1986) Quantitative cytoarchitectonics of the posterior cingulate cortex in primates. J. Comp. Neurol. *253:*514–524.